

# Millimeter-Wave Antenna Design Inspired by Half-Ring Resonators for 5G Communication Systems

Caner Murat  
Electrical and Electronics  
Engineering  
Recep Tayyip Erdogan University  
Rize, Turkey  
caner.murat@erdogan.edu.tr

Mohammad Alibakhshikenari  
Electronics Engineering  
Department,  
University of Rome "Tor  
Vergata"  
00133 Rome, Italy  
alibakhshikenari@ing.uniroma2.it

Peiman Parand  
Electronics Engineering  
Department  
University of Rome "Tor  
Vergata"  
00133 Rome, Italy  
peiman.parand@students.uniroma2.eu

Hassan Zakeri  
Department of Electrical  
Engineering  
Amirkabir University of  
Technology (Tehran Polytechnic)  
Tehran 158754413, Iran  
h.zakeri@aut.ac.ir

Reza Afroozeh  
Department of Electrical  
Engineering  
Shahed University  
Tehran, Iran  
rezaafroozeh@shahed.ac.ir

Bal Virdee  
Center for Communications  
Technology  
London Metropolitan University  
London N7 8DB, UK  
b.virdee@londonmet.ac.uk

Lida Kouhalvandi  
Department of Electrical and  
Electronics Engineering  
Dogus University  
Istanbul 34775, Turkey  
lida.kouhalvandi@ieec.org

Patrick Longhi  
Electronics Engineering  
Department  
University of Rome "Tor  
Vergata"  
00133 Rome, Italy  
longhi@ing.uniroma2.it

Ernesto Limiti  
Electronics Engineering Department  
University of Rome "Tor Vergata"  
00133 Rome, Italy  
limiti@ing.uniroma2.it

Corresponding Author: Mohammad Alibakhshikenari

**Abstract**—The proposed antenna design incorporates half-ring resonators with radiation properties that are contingent upon the line thickness and gap spacing. The symmetrical spring segments situated at the horizontal centerline directs the bidirectional radiation. The bottom surface of the FR4 substrate, coated with 35  $\mu\text{m}$  of copper, acts as a reflector for electromagnetic (EM) waves, thereby increasing the intensity of the waves in accordance with the principles of image theory. The simulation results demonstrate that the antenna achieves a return loss of  $-30.3$  dB at 33 GHz, covering a bandwidth of 2.3 GHz, which is sufficient for 5G applications through millimeter-wave (mm-wave domain). To prevent system noise, the additional increase in bandwidth is avoided. The antenna exhibits high performance, with a maximum gain of 10 dBi at  $\phi=0^\circ$  and  $\theta=0^\circ$ , 4.04 dBi at  $\phi=90^\circ$ , and a directivity of 12.85 dBi at 33 GHz. The far-field radiation patterns exhibit half-power beamwidths of  $17.4^\circ$ ,  $22.5^\circ$ , and  $25.3^\circ$  in the azimuth and elevation planes, respectively. The proposed mm-wave antenna structure offers high gain and directivity, rendering it an optimal choice for efficient, low-loss data transmission in 5G applications. The optimized impedance matching and minimized reflection losses serve to further enhance the antenna's performance, thereby meeting the stringent demands of modern communication systems.

**Keywords**—mm-Wave antenna, half-ring resonators, 5G applications, bidirectional communications, EM-waves.

## I. INTRODUCTION

The recent advancements within the domain of wireless communication technology have given rise to an imperative need for enhanced performance and extended capabilities within wireless systems. A significant technological advancement that is driving the development of fifth generation (5G) mobile wireless communication systems is the utilization of the mm-wave band, which is renowned for providing an exceedingly broad bandwidth as well as high-speed and efficient data transfer capabilities. [1-4].

Millimeter-wave communication enables wide bandwidth, ultra-fast data transmission, and minimal latency. As demand grows for lightweight and flexible electronics in smart homes and wearables, solutions that minimize metal content and rigidity while using less material are needed [5,6]. Nevertheless, difficulties such as significant propagation attenuation and considerable signal losses still exist. The use of antenna arrays is an effective method of reducing the effects of high path losses in millimeter-wave systems [7].

In this study, a ring resonator-based microstrip patch antenna structure is selected for the realization of millimeter-wave electromagnetic radiation. The design of efficient, concentrated and broad-spectrum antennas for millimeter-wave

communication systems represents a significant area of research. For this purpose, the array antenna configuration is deemed an appropriate choice for this study, given its capacity to accumulate numerous high-gain, compact radiation patterns based on ring resonators, which can be employed to manipulate electromagnetic waves. Array antenna structures have the potential to markedly enhance antenna performance in comparison to single-patch antennas [8-11]. In the proposed work, an antenna design that is well-suited for 5G applications is realized by leveraging the advantages inherent to these structures.

Recent studies in the field have explored various innovative designs to meet the demands of 5G applications indicated in Table 1. In 2018, Jilani et al. introduce an inkjet-printed mm-wave flexible antenna for 5G, emphasizing the use of a Polyethylene Terephthalate substrate [12]. Abbas et al. discuss a MIMO antenna system that integrates mm-wave 5G and 4G antennas in the same structure, offering a unique design proposition in 2019 [13]. Kurvinen et al. propose a plastic enclosure insulating metal parts of antennas to reduce interference, a crucial strategy for interference mitigation in 2020 [14]. Within the same year, Alkaraki & Gao introduce low-cost 3D printed MIMO antennas with beam switching capabilities for 5G [15]. Khalid et al. analyze a 4-port MIMO antenna with a defected ground structure for 5G mm-wave applications, evaluating its MIMO performance metrics in the same year [16]. In 2022, Khan et al. present a mm-wave MIMO antenna array for 5G communication terminals [17]. Cao et al. develop a mm-wave broadband MIMO antenna using metasurfaces for 5G, focusing on compact size and high performance in 2023 [18]. Shetty discusses a miniaturized hexagonal antenna with a defected ground plane for 5G mm-wave applications, exploring current trends and fabrication technologies in 2023 [19]. Masood introduces an ultra-wideband antenna for future mm-wave applications, emphasizing the synergy between UWB and mm-wave technology in the same year [20]. According to Table 1, the proposed work offers a more advantageous antenna gain in comparison to the existing studies. The design details of the proposed antenna are presented in Section 2, the corresponding simulation studies are outlined in Section 3, comparison of state of art mm wave antenna design with proposed half ring resonator-based antenna are in Section 4 and a concluding paragraph is provided in Section 5.

TABLE I. STATE OF ART MM WAVE ANNTENNA PERFORMANCES

References	Year	Freq. [GHz]	S <sub>11</sub> [dB]	Gain [dBi]	Size [mm <sup>2</sup> ]
[12]	2018	39	-20	7.44	13×8
[13]	2019	38	-35	9.14	70×78
[14]	2020	27	-10	N.A	2×5
[15]	2020	36.5	-30	9.7	16×19
[16]	2020	28	-40	8.3	30×35
[17]	2022	37	-23	12.8	10×6
[18]	2023	28	-30	9.4	20×20
[19]	2023	42	-60	6.5	9×5
[20]	2023	40	-10	7	5×7
<b>This work</b>	<b>2024</b>	<b>33</b>	<b>-30.3</b>	<b>10</b>	<b>15×15</b>

## II. DESIGN OF PROPOSED STRUCTURE

Figure 1 presents a geometric view of the proposed antenna structure. The antenna is constituted by the combination of three identical half-ring resonators for electromagnetic radiation. The radiation properties of each half-ring resonator are dependent on the line thickness (W2) and the gap between them (W3). At the horizontal center line of the antenna, where the half-ring resonators converge, there are spring segments that are symmetrical to the vertical axis and gradually increase in length. These arc segments determine the radiation direction, resulting in bidirectional radiation.

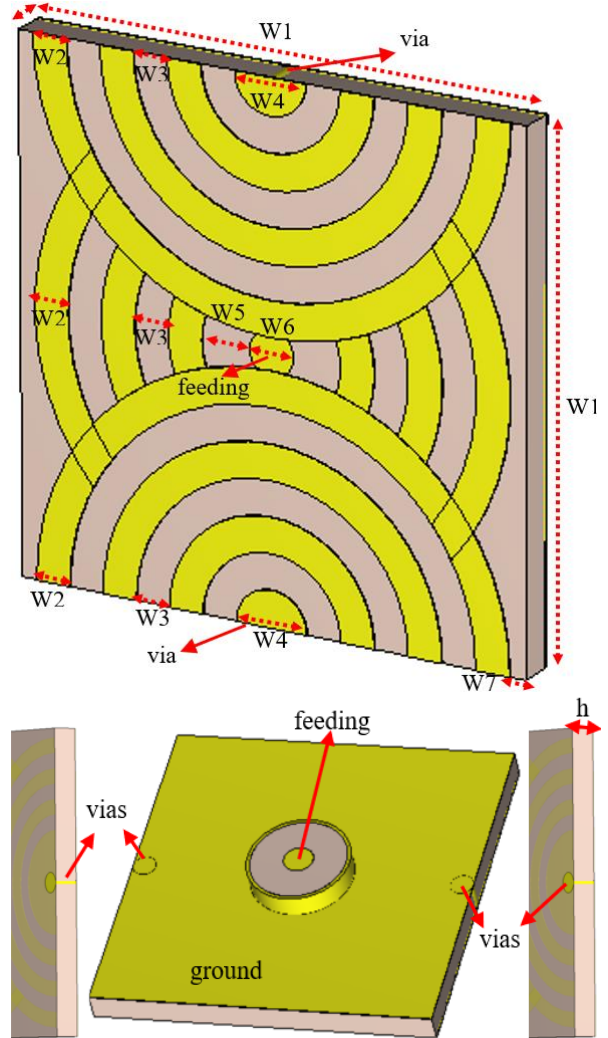


Fig.1. Proposed mm-wave antenna geometry.

represented by W5, represents the region where the waveguide port is located. The mentioned antenna dimensions are given in Table 2.

The bottom surface of the FR4 antenna substrate material, as illustrated in Figure 1, is coated with 35  $\mu\text{m}$  of copper. Given that this copper surface constitutes the ground part, it reflects the

electromagnetic waves back in accordance with the image theory, thereby increasing the intensity of the waves in the radiation direction. The circle situated at the centre of the antenna, represented by the diameter length  $W_6$ , represents the positive end of the antenna feed. The region surrounding this,

TABLE II. DESIGN PARAMETERS OF PROPOSED ANTENNA

Dimensions	W1	W2	W3	W4	W5	W6	W7	H
Value [mm]	15	0.75	1	2.1	4.2	1.3	0.5	1

### III. NUMERICAL CALCULATION AND DATA COLLECTION

The ring resonator-based mm-wave antenna design has been simulated using Finite Integration Technique with 72,576 mesh cells in CST Microwave Studio. The reflection coefficient obtained from the simulation is presented in Figure 2. Based on the data obtained, the antenna's operating bandwidth has been identified to lie between 33.9 GHz and 36.2 GHz. These findings demonstrate that the antenna demonstrates efficacy at mm-wave frequencies.

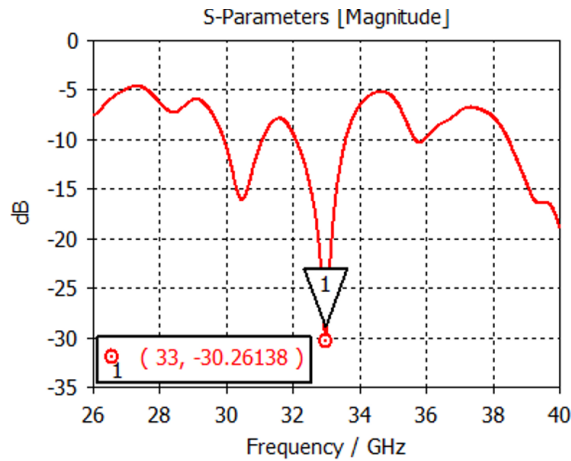
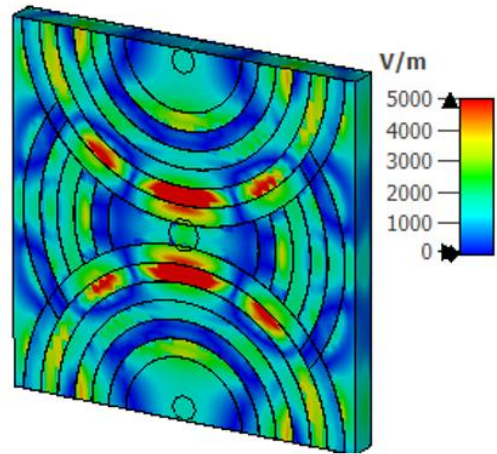


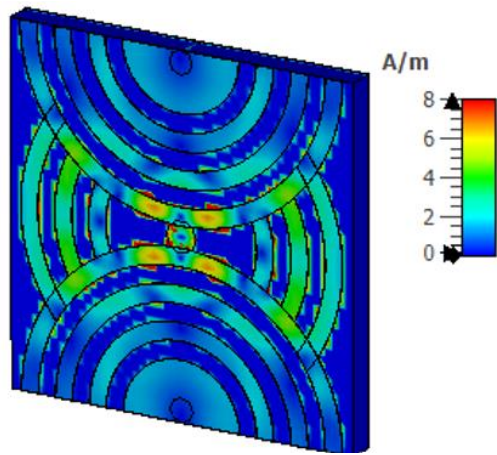
Fig.2. S parameters of proposed antenna.

Figure 2 illustrates the return loss of the ring resonator based proposed antenna, which is -30.26 dB at 33 GHz. This value encompasses a bandwidth of 2.3 GHz in the mm-wave wavelength range. This bandwidth is sufficient for utilization in 5G applications. However, it is preferable to avoid increasing the bandwidth further, as this may result in an increase in noise within the system.

In Figure 3, the surface current and electric field distribution is indicated. The current surface distribution peaks at 8 A/m, with strong resonance near specific antenna regions, particularly around the feed point, indicating efficient radiation generation. The E-field distribution, reaching up to 5 kV/m, aligns with these current hotspots, showing strong coupling between currents and radiated fields. The symmetry in both distributions suggests efficient radiation, though minor non-uniformities could hint at potential side lobes or bandwidth limitations. Together, these images confirm the antenna operates near resonance, optimizing electromagnetic wave radiation.



(a)

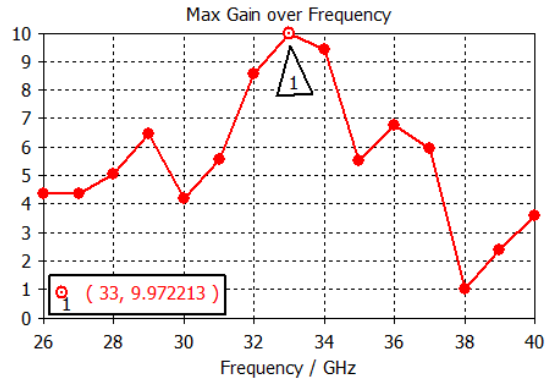


(b)

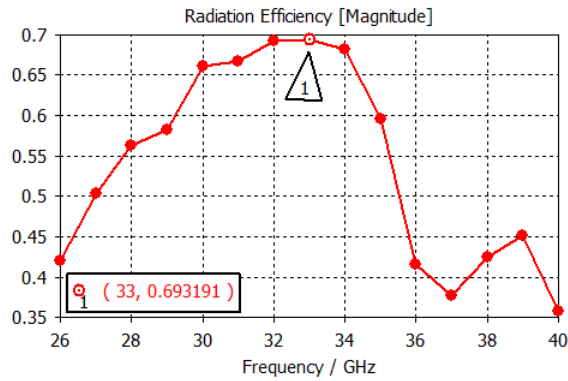
Fig.3. (a) Electric field and (b) surface current distribution of half ring resonator based mm wave antenna

Minor non-uniformities in the distributions indicated in Figure 3 may indicate the potential for side lobe formation or constraints in the antenna's operational bandwidth. These slight irregularities could be linked to geometrical factors or material properties that influence the field patterns. Overall, the observations from Figure 3 confirm that the antenna operates near a resonant mode, where its design parameters, such as geometry and materials, are optimized for efficient electromagnetic wave radiation. This resonant operation is critical for achieving high performance in terms of gain, directivity, and radiation efficiency.

Figure 4 depicts the variation of the maximum gain and radiation efficiency of an antenna over a frequency range from 26 GHz to 40 GHz. Figure 4.a displays the radiation efficiency, while Figure 4.b showcases the maximum gain. These two metrics are critical in assessing the effectiveness and reliability



(a)



(b)

Fig.4. (a) Maximum gain and (b) radiation efficiency over frequency graphs of proposed antenna

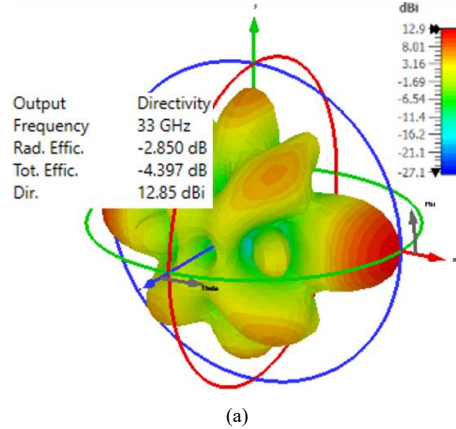
of the system at different frequencies. The analysis of these parameters provides insights into the antenna's operational characteristics, highlighting the frequencies where it performs most efficiently and effectively, as well as identifying areas where performance diminishes due to system limitations or external factors. This understanding is essential for optimizing the antenna's design and application in practical scenarios.

In Figure 4.a, the gain initially peaks at around 28 GHz before dropping to a local minimum of 4 dB at 30 GHz, likely due to impedance mismatches or system losses. It then rises sharply to a maximum of 9.97 dBi at 33 GHz, the system's optimal operating frequency, where resonance and impedance matching maximize performance. Beyond 33 GHz, the gain declines rapidly, reaching 5 dB by 35 GHz, indicating reduced efficiency and resonance loss. From 35 GHz to 40 GHz, fluctuations suggest secondary resonances or higher-order modes, with a consistent drop near 40 GHz highlighting the system's operational limits and increasing losses.

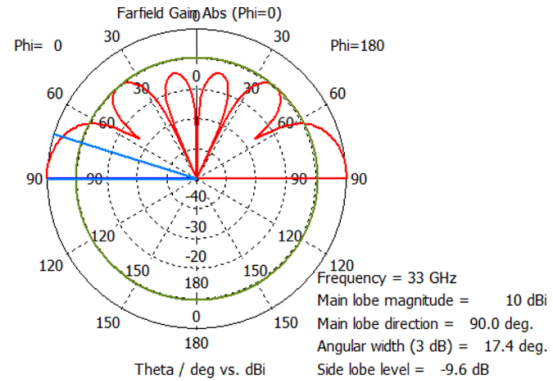
In Figure 4.b, the efficiency is approximately 0.42 at 26 GHz and steadily increases, reaching its maximum value of 0.693 at 33 GHz, which marks the system's optimal performance in terms of energy radiation. Beyond this peak, the efficiency begins to decline sharply, dropping below 0.4 by 37 GHz and falling to its lowest point, nearly 0.35, at 40 GHz. This trend suggests that the system operates effectively around 33 GHz, with significant

losses in radiation efficiency at higher frequencies. The sharp drop in efficiency post-33 GHz may indicate design or material limitations that reduce performance at higher frequencies, emphasizing the need to focus on the lower frequency range for optimal operation.

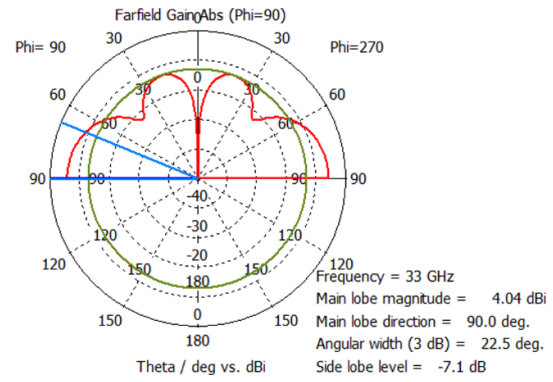
Following the numerical calculation of the S parameters and 2D field distributions of the ring resonator-based antenna having minimum at 33 GHz, the directivity and gain simulations are evaluated at that frequency. Figure 5.a illustrates the far field results in 3D view, while Figures 5.b, 5.c and 5.d depict in azimuth and elevation plane at angles  $\varphi = 0^\circ$ ,  $\varphi = 90^\circ$  and  $\theta = 0^\circ$ , respectively.



(a)



(b)



(c)

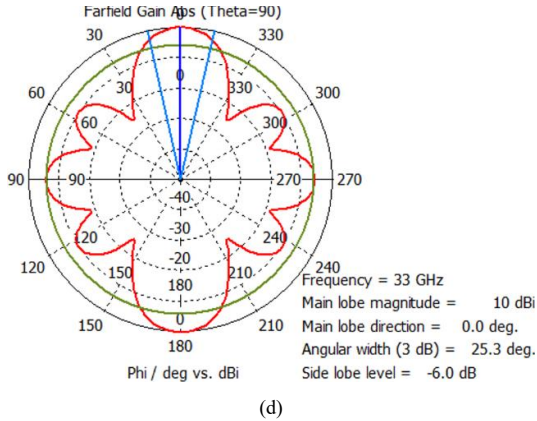


Fig.5. (a) 3D directivity, and (b – d) the axial gain values of proposed mm-wave antenna at 33 GHz when  $\varphi = 0^\circ$ ,  $\varphi = 90^\circ$ , and  $\theta = 0^\circ$ , respectively.

The proposed ring resonator-based antenna exhibits a superior directivity level of 12.85 dBi at the excitation frequency of 33 GHz, as illustrated in Figure 5.a. This remarkable directive performance aligns it well with the requirements of mm-wave applications that necessitate low-loss data transfer in desired direction. Moreover, Figures 5.b to 5.d demonstrate the antenna's maximal gain at 33 GHz operating frequency. Gain values of up to 10 dBi at  $\varphi=0^\circ$  and  $\theta=0^\circ$ , 4.04 dBi at  $\varphi=90^\circ$  are achieved with proposed design. Furthermore, the far-field gain simulation results presented in Figures 5.b to 5.d illustrate a half-power beam width (HPBW) of  $17.4^\circ$ ,  $22.5^\circ$  and  $25.3^\circ$ , respectively. The values indicate that the proposed ring resonator-based mm-wave antenna provides bidirectional radiation with high gain, which is highly advantageous for communication in the 5G band.

#### IV. COMPARISON

Table 1 presents a detailed comparison of the proposed antenna with recently published works, evaluating key performance metrics such as operating frequency, return loss ( $S_{11}$ ), gain, and physical size. The proposed antenna, operating at 33 GHz, achieves a return loss of -30.3 dBi and a peak gain of 10 dBi, while maintaining a compact size of  $(15 \times 15 \text{ mm}^2)$ . This combination of high gain and small size highlights the advantages of the proposed design compared to existing antennas in the same frequency range.

In terms of gain, the proposed antenna demonstrates superior performance compared to several prior works. For instance, [12] achieves a gain of 7.44 dBi at 39 GHz, while [20] achieves a gain of 7 dBi at 40 GHz, both of which are lower than the 10 dBi achieved by the proposed antenna. Furthermore, designs such as [16] and [18] achieve gains of 8.3 dBi and 9.4 dBi at 28 GHz, respectively, but their larger sizes ( $30 \times 35 \text{ mm}^2$  and  $20 \times 20 \text{ mm}^2$ ) indicate a trade-off between size and gain. The proposed design offers a higher gain than these works, with a more compact structure compared to [16] and comparable size to [18].

When compared to designs with high gain, such as [13], [15], and [17], which achieve gains of 9.14 dBi, 9.7 dBi, and 12.8 dBi, respectively, the proposed antenna maintains a competitive balance between performance and size. Although [17] achieves the highest gain of 12.8 dBi, it operates at 37 GHz and has a

smaller size of  $10 \times 6 \text{ mm}^2$ , which may limit its bandwidth or efficiency. In contrast, the proposed antenna offers a slightly lower gain but operates at a lower frequency of 33 GHz, which is advantageous for applications requiring lower propagation losses and better material penetration. Similarly, [15] achieves a comparable gain of 9.7 dBi at 36.5 GHz with a size of  $16 \times 9 \text{ mm}^2$ , slightly larger than the proposed design.

The return loss of the proposed antenna is also among the best in the comparison. With a value of -30.3 dBi, it demonstrates excellent impedance matching and minimal reflection, outperforming designs such as [14] (-10 dBi), [12] (-20 dBi), and [17] (-23 dBi). Only [19], with a return loss of -60 dBi at 42 GHz, and [16] (-40 dBi at 28 GHz) offer better impedance matching, but they either operate at a higher frequency or exhibit a larger size, making them less suitable for applications requiring compact designs at mid-millimeter-wave frequencies.

Regarding physical size, the proposed design achieves a good trade-off between compactness and performance. Designs such as [14] ( $2 \times 5 \text{ mm}^2$ ) and [19] ( $9 \times 5 \text{ mm}^2$ ) are much smaller but suffer from either unavailable gain values or significantly lower gain (6.5 dBi for [19]). In comparison, designs such as [13] ( $70 \times 78 \text{ mm}^2$ ) and [16] ( $30 \times 35 \text{ mm}^2$ ) are substantially larger, which may limit their integration into compact devices. The proposed antenna, with its moderate size of  $15 \times 15 \text{ mm}^2$ , offers a balanced solution for applications requiring both compactness and high performance.

In summary, the proposed antenna achieves an optimal combination of high gain, excellent impedance matching, and compact size. It outperforms many of the referenced designs in gain and return loss, while maintaining a size that is suitable for modern millimeter-wave applications such as 5G, radar systems, and point-to-point communication. This demonstrates the effectiveness of the proposed design in addressing the challenges of high-frequency antenna development.

#### V. CONCLUSION

The proposed millimeter-wave antenna has been demonstrated to fulfil the requisite specifications for high gain and bandwidth in 5G applications. The design incorporates three identical half-ring resonators, with the direction of radiation being influenced by the line thickness and the gap spacing. The simulation results demonstrate a  $S_{11}$  of -30.26 dB at 33 GHz and a 2.3 GHz bandwidth, which is appropriate for 5G applications. Subsequent bandwidth increments are precluded to circumvent the introduction of noise. At 33 GHz, the antenna exhibits minimal reflection loss, exhibiting gain of 10 dBi at  $\varphi = 0^\circ$  and  $\theta = 0^\circ$ , 4.04 dBi at  $\varphi = 90^\circ$ , and 12.85 dBi directivity value. In conclusion, the proposed ring resonator-based mm-wave antenna offers high gain and directivity, rendering it an optimal choice for 5G applications that necessitate efficient, low-loss data transmission. Optimized impedance matching and minimized reflection losses serve to further enhance its performance, meeting the exacting demands of modern communication systems.

## REFERENCES

- [1] W. Hong, K. H. Baek, and S. Ko, "Millimeter-wave 5G antennas for smartphones: overview and experimental demonstration," *IEEE Trans. Antennas Propag.*, vol. 65, no. 12, pp. 6250-6261, 2017.
- [2] Zakeri, Hassan, et al. "A Compact Dual Circularly Polarized MIMO Antenna with Controlled Slots for 5G Wireless Applications Across mm-Wave Spectrum", 17th United Conference on Millimetre Waves and Terahertz Technologies (UCMMT), pp. 194-198, Palermo, Italy, 21- 24 August, 2024.
- [3] Khorasani, Seyed Ali, et al. "Orbital angular momentum with the approach of using in sub-6GHz 5G mobile communications for wireless applications." 6<sup>th</sup> Global Power, Energy and Communication Conference (GPECOM), pp. 800-803, Budapest, Hungary, 04-07 June 2024.
- [4] Z. Qu, S. W. Qu, Z. Zhang, S. Yang, and C. H. Chan, "Wide-angle scanning lens fed by small-scale antenna array for 5G in millimeter-wave band," *IEEE Trans. Antennas Propag.*, vol. 68, no. 5, pp. 3635–3643, 2020.
- [5] Zakeri, Hassan, et al. "Low-cost multiband four-port phased array antenna for sub-6 GHz 5G applications with enhanced gain methodology in radio-over-fiber systems using modulation instability", *IEEE Access*, vol. 12, pp. 117787-117799, 2024.
- [6] T. S. Rappaport, Y. Xing, G. R. MacCartney, A. F. Molisch, E. Mellios and J. Zhang, "Overview of Millimeter Wave Communications for Fifth-Generation (5G) Wireless Networks—With a Focus on Propagation Models," in *IEEE Transactions on Antennas and Propagation*, vol. 65, no. 12, pp. 6213-6230, Dec. 2017.
- [7] Zakeri, Hassan, et al. " Path Loss Model Estimation at Indoor Environment by Using Deep Neural Network and CatBoost for Wireless Application", *IEEE Access*, vol. 12, pp. 159070-159085, 2024.
- [8] Khoddami, Parsa, et al. "THz Antenna Assisted by Graphene for 6G Communications", 17<sup>th</sup> United Conference on Millimetre Waves and Terahertz Technologies (UCMMT), pp. 151-155, Palermo, Italy, 21- 24 August, 2024.
- [9] W. Yang, D. Chen and W. Che, "High-efficiency high-isolation dual-orthogonally polarized patch antennas using nonperiodic RAMC structure," *IEEE Trans. Antennas Propag.*, vol. 65, no. 2, pp. 887-892, Feb. 2017.
- [10] D. Chen, W. Yang and W. Che, "High-gain patch antenna based on cylindrically projected EBG planes," *IEEE Antennas Wireless Propag. Lett.*, vol. 17, no. 12, pp. 2374-2378, Dec. 2018.
- [11] S. X. Ta, I. Park, "Low-profile broadband circularly polarized patch antenna using metasurface," *IEEE Trans. Antennas Propag.*, vol. 63, no. 12, pp. 5929-5934, Dec. 2015.
- [12] Jilani, Syeda Fizzah, Qammer H. Abbasi, and Akram Alomainy. "Inkjet-printed millimetre-wave PET-based flexible antenna for 5G wireless applications." *IEEE*, 2018.
- [13] Al Abbas, Emad, et al. "MIMO antenna system for multi-band millimeter-wave 5G and wideband 4G mobile communications." *IEEE Access* 7 (2019): 181916-181923.
- [14] Kurvinen, Joni, et al. "Capacitively-loaded feed line to improve mm-wave and sub-6 GHz antenna co-existence." *IEEE Access* 8 (2020): 139680-139690.
- [15] Alkaraki, Shaker, and Yue Gao. "Mm-wave low-cost 3D printed MIMO antennas with beam switching capabilities for 5G communication systems." *IEEE access* 8 (2020): 32531-32541.
- [16] Khalid, Mahnoor, et al. "4-Port MIMO antenna with defected ground structure for 5G millimeter wave applications." *Electronics* 9.1 (2020): 71.
- [17] Khan, Jalal, et al. "Design of a millimeter-wave MIMO antenna array for 5G communication terminals." *Sensors* 22.7 (2022): 2768.
- [18] Cao, Thanh Nghia, et al. "Millimeter - Wave Broadband MIMO Antenna Using Metasurfaces for 5G Cellular Networks." *International Journal of RF and Microwave Computer - Aided Engineering* 2023.1 (2023): 9938824.
- [19] Shetty, Ramya, et al. "Miniaturized Hexagonal Antenna with Defected Ground Plane for 5G mm Wave Applications." *Progress in Electromagnetics Research C* 137 (2023).
- [20] Masood, Asad, and N. Nizam-Uddin. "An Ultra-wideband Antenna for Future mm-Wave Applications." (2023).